

Fig. 1. UV-vis absorption spectra of PVA/SA and PVA/SA/Ag films at different Ag^+ ion concentrations at 15 kGy gamma irradiation dose.

3.2. XRD analysis

Fig. 3 shows the XRD patterns of pure PVA and PVA/SA films. The XRD of pure PVA exhibits a strong peak at $2\theta = 19.57^\circ$ with a shoulder at $2\theta = 22.97^\circ$. The peak at $2\theta = 19.57^\circ$ corresponds to the (110) reflection, a plane which contains the extended planar zig-zag chain direction of the crystallites. The shoulder peak at $2\theta = 22.97^\circ$ is related to the reflection from the plane (200). Also, PVA film shows two weaker peaks at $2\theta = 11.02^\circ$ and 40.42° . Upon addition of amorphous sodium alginate to polyvinyl alcohol, the intensity of the diffraction peak at $2\theta = 19.57^\circ$ becomes lower showing that the crystallinity of PVA/SA film is lower than that of pristine PVA film. The reduction of crystallinity of PVA/SA film is the diluting effect of amorphous sodium alginate PVA/SA blend and indeed the crystallinity of PVA remains effectively unchanged as shown by DSC measurements in Table 1.

Fig. 4 displays X-ray diffraction patterns of the PVA/SA/Ag composite films with different silver nitrate concentrations. The composites containing silver nitrate show five new diffraction peaks at $2\theta = 38.1, 44.2, 64.4, 77.2$ and 81.3° more clearly in curve c. The reflection peaks can be indexed to the planes (111), (200), (220), (311) and (222), respectively, corresponding to

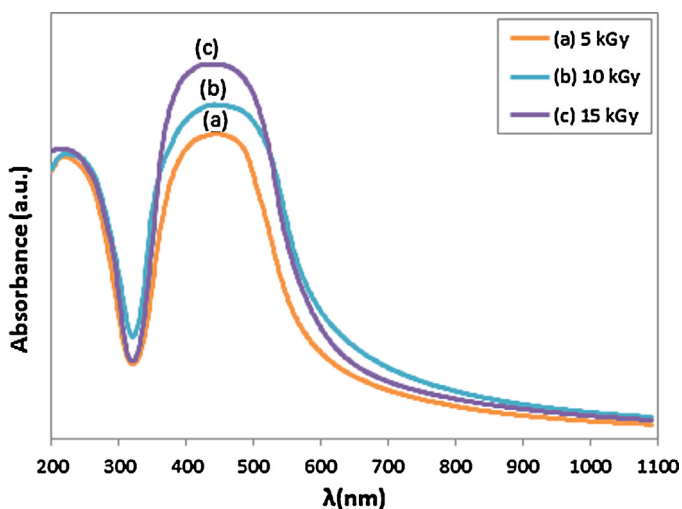


Fig. 2. UV-vis absorption spectra of PVA/SA/Ag composites at different gamma irradiation doses at a fixed Ag^+ ion concentration of 1.33 wt.%.

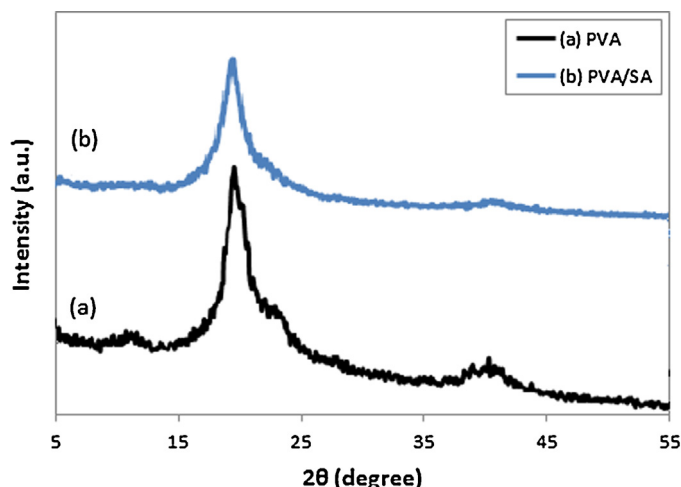


Fig. 3. XRD patterns of PVA and PVA/SA.

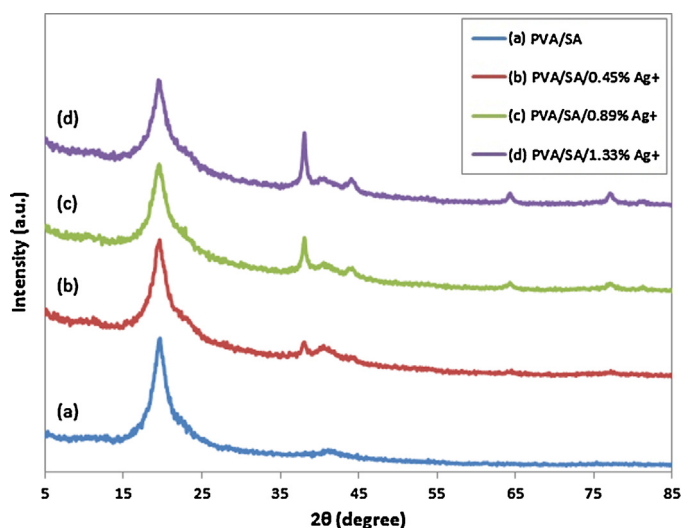


Fig. 4. XRD patterns of PVA/SA film and PVA/SA/Ag composite films at different concentrations of Ag^+ ion irradiated at 15 kGy dose.

face-centered cubic structure of silver according to JCPDS (No. 4-0783). As shown in Fig. 4 with increasing silver ion concentration irradiated at 15 kGy, the intensity of the corresponding Ag peaks increased.

Fig. 5 shows XRD spectrum of PVA/SA/Ag composite with Ag^+ ion concentration of 1.33 wt.% at different gamma irradiation doses. By increasing gamma irradiation dose intensity of Ag peaks at $2\theta = 38.1, 44.2, 64.4, 77.2$ and 81.3° increased due to increase in the number of silver particles.

3.3. DLS analysis

DLS size distribution of Ag nanoparticles is shown in Fig. 6. The distribution was quite narrow and the particle diameters ranged from 43.8 up to 164 nm with an average size of 69.8 nm. Only 7.3%

Table 1
Melting point and crystallinity of PVA/SA/Ag composites.

Sample	Melting temp. $^\circ\text{C}$	Crystallinity %
PVA	223.6	33.7 ± 0.2
PVA/SA	222.1	33.4 ± 0.2
PVA/SA/0.45 Ag^+	220.4	33.2 ± 0.2
PVA/SA/0.89 Ag^+	219.5	32.8 ± 0.2
PVA/SA/1.33 Ag^+	218.0	31.8 ± 0.2

Table 2
Tensile modulus and elongation at break of PVA and PVA/SA films.

Sample	Tensile modulus (MPa)	Tensile strength (MPa)	Elongation at break (%)
PVA	500	42	152
PVA/SA	710	45	56

Table 3
Tensile modulus and elongation at break of PVA/SA/1.33% Ag⁺ ion nanocomposite at various gamma irradiation doses.

Dose	Tensile modulus (MPa)	Tensile strength (MPa)	Elongation at break (%)
5	570	36	42
10	610	38	25
15	650	47	22

Table 4
Variation of the inhibition zone (mm) with silver concentration and gamma irradiation dose.

Sample	<i>E. coli</i>	<i>S. aureus</i>
PVA/SA/0.45Ag ⁺ /15kGy	2.5	1.5
PVA/SA/0.89Ag ⁺ /15kGy	2.8	1.8
PVA/SA/1.33Ag ⁺ /15kGy	3.2	2.1
PVA/SA/1.33Ag ⁺ /10kGy	2.5	1.5
PVA/SA/1.33Ag ⁺ /5kGy	1.5	1

with very small decrease in crystallinity of PVA. The decrease in crystallinity is attributed to decrease in intermolecular hydrogen bonding between PVA molecular chains.

3.6. Mechanical properties

Table 2 shows that PVA film is a strong and flexible polymer with modulus, strength and elongation at break of about 500 MPa, 42 MPa and 152%, respectively. Sodium alginate is a rigid polymer with high modulus that upon addition to polyvinyl alcohol increased the modulus and strength along with decrease in elongation. In spite of the reduction in the flexibility of PVA the resulting PVA/SA blend is strong enough with reasonable flexibility for most applications. Although addition of silver nanoparticles at 1.33% level results in a moderate reduction in mechanical properties compared to PVA/SA blend (Table 3), however the reduction in the modulus and strength is recovered at higher doses of gamma irradiation. This could be attributed to the smaller size and larger number

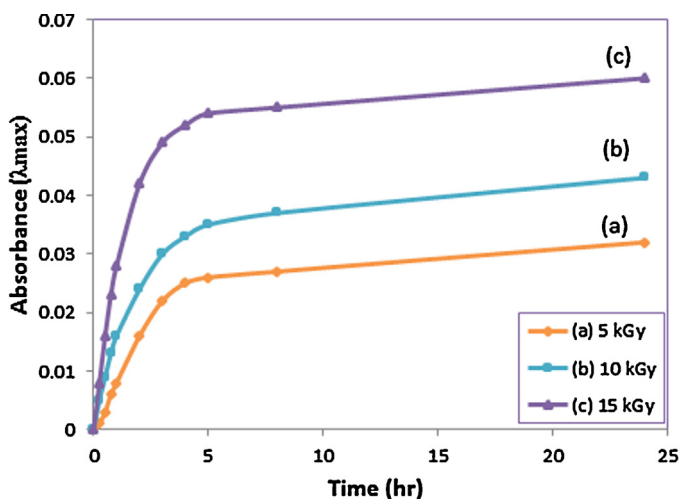


Fig. 9. Release of silver from composites at different doses of gamma irradiation and Ag⁺ ion concentration of 1.33 wt.%.

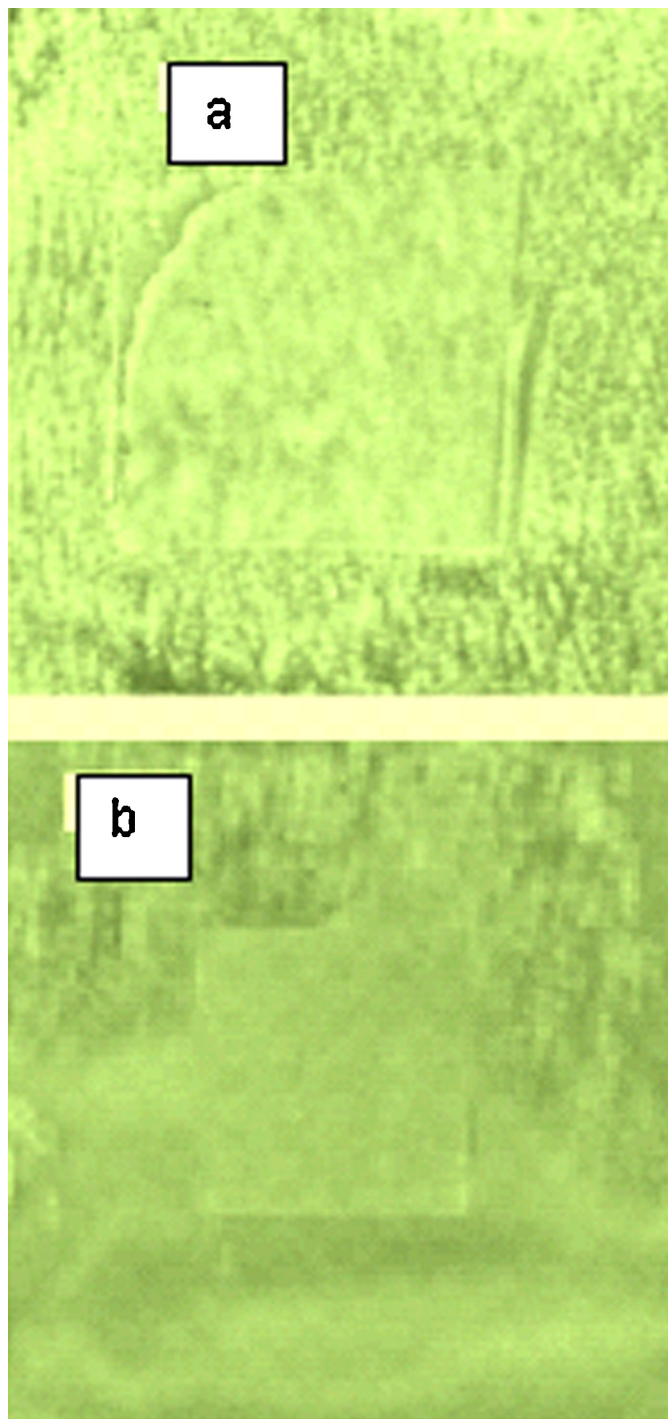


Fig. 10. Images of antibacterial activity of PVA/SA films: (a) *S. aureus* and (b) *E. coli*.

of the silver nanoparticles produced at higher doses. It could be envisaged that smaller nanoparticles could develop stronger interactions with the matrix of PVA/SA blend and boost rigidity and strength of the PVA/SA blend. Also the larger number of nanoparticles produced at higher doses led to a loss in elongation.

3.7. Release of silver from composite films

Fig. 9 shows release of silver from PVA/SA/Ag composite film at various gamma irradiation doses and Ag⁺ ion concentration of 1.33 wt.%. As shown the release rate of silver in the early hours was rapid but after about 5 h the rate slowed down and approached